**Akash T. Jadhav**
Engineering Student
Department of Aeronautical Engineering
AnnaSaheb Dange College of Engineering & Technology, Ashta
India

**Payal V. Tembhurnikar**
Engineering Student
Department of Aeronautical Engineering
AnnaSaheb Dange College of Engineering & Technology, Ashta
India

**Mrunal S. Bhosale**
Engineering Student
Department of Aeronautical Engineering
AnnaSaheb Dange College of Engineering & Technology, Ashta
India

**Jhumki Nandy**
Assistant Professor
Department of Aeronautical Engineering
Nitte Meenakshi Institute of Technology
Bangalore, India

**MD Gulam Sarwar**
Assistant Professor
Hypersonic Experimental Aerodynamics Laboratory (HEAL), Department of Aerospace Engineering, Indian Institute of Technology Kanpur, Uttar Pradesh, India

**Devabrata Sahoo**
Associate Professor
Department of Aerospace Engineering
Graphic Era (Deemed to be University)
Dehradun,
India

# Effect of Size and Location of an Intermediate Aerodisk Mounted Sharp Tip Spike on the Drag Reduction over a Hemispherical Body at Mach 2.0

*To minimize forebody drag in high-speed flying vehicles such as missiles and rockets, contemporary research has focused on computational methods to analyze drag reduction strategies. This study investigates the efficacy of an intermediate aerodisk mounted on a sharp-tip spike at a Mach number of 2.0. Through a parametric analysis, variations in aerodisk size and location on the spike stem are explored. Results indicate that reducing the size of the intermediate aerodisk to 3 mm maintains identical reattachment shock strength but leads to higher pressure values at the transition from separation shock to reattachment shock. The model with an expanded 5 mm aerodisk size exhibits the second-lowest peak pressure coefficient for reattachment shock, suggesting improved flow recirculation and lower heating levels. Conversely, a 6 mm aerodisk size increases reattachment shock pressure but enhances flow recirculation, impacting total drag. Overall, the study concludes that an intermediate aerodisk, particularly with a 5 mm diameter, provides an optimal configuration for drag reduction before flow separation.*

***Keywords:*** *Supersonic flow, Drag reduction, Spike, Aerodisk.*

## 1. INTRODUCTION

The aviation industry is bringing its vision to the field of supersonic flying vehicles. The supersonic field of study has accounted for many advancements throughout the decades and, with no doubt, challenges to overcome. For high-speed operations, blunt bodies are chosen instead of conical bodies because of their volumetric efficiency and effective heating load distribution. The only downfall blunt bodies have is the overall increased drag they experience. To counter this downfall, 'spike' found its way into this research field. In the past half a century, many researchers have shown interest in studying the dynamics of spike and blunt body combinations operating at high speeds. The advantage of providing a blunt body with a spike at supersonic speed is it can modify the flow physics around the body, resulting in a reduced forebody drag [1]. Figure 1 showcases the schematic representation of the change in flow physics over a hemispherical body while mounting a typical spike.

A clean, blunt body kept in a supersonic flow will experience a strong detached bow shock in front of it. Spike protruding from the point of stagnation on a blunt body replaces the intense bow shock wave with a system of comparatively weaker oblique shocks. The system of shock wave generated includes the leading edge shock observed at the spike tip, a separation shock observed to be generated at the point of flow separation over the spike stem, and the reattachment shock observed at the flow reattachment point over the surface of the blunt body. This replacement of the shock system increases the drag reduction over the body to a considerable extent. A region of recirculation is seen to form around the interface between the spike and the forebody, enclosed by the shear layer separated from the external flow. The recirculation zone is effective in normalizing the heating. As weaker oblique shock waves replace the strong bow shock, the pressure levels along the blunt body surface reduce, and this reduction in the pressure level then results in a reduction in the forebody drag experienced by the spiked body. Ahmed and Qin [2] reviewed the research works exploring the decrease in drag force experienced by the blunt body at high speeds by mounting a spike on the stagnation point, which various researchers have investigated and reported.

In the past, numerous researchers studied the parametric effects of spikes on the drag reduction for hemispherical bodies moving in supersonic airframes [3-

Received: April 2024, Accepted: May 2024
Correspondence to: Dr Devabrata Sahoo, Associate Professor, Department of Aerospace Engineering, Graphic Era (Deemed to be University), Dehradun,India
E-mail: devtapu@gmail.com
**doi: 10.5937/fme2403419J**

8]. Jones [3] investigated the efficacy of spike length concerning the operating Mach and reported that if spike length is within the critical length, significant drag reduction is achieved. The ratio of the spike length (L) to the diameter of the main body (D), which marks the critical spike length offering a maximum reduction in drag, was reported as L/D=1.5. Further, researchers reported the effectiveness of an aerodisk as mounting an aerodisk at the spike tip location leads to a further increase in drag reduction compared to a sharp tip spike [9,10]. When the aerodisk replaces the sharp tip of the spike, the recirculation zone is observed to increase in size, thereby reducing the strength of reattachment shock. This results in a decrease in surface pressure levels, and thus, a reduction in drag coefficient is obtained. Computational studies performed by Yadav et al. [11,12] at hypersonic speed suggested that by mounting a series of aerodisks along the spike stem rather than a single aerodisk mounted on the spiked body configuration, further drag reduction can be achieved. However, all the studies mentioned above focusing on enhancing drag reduction over spiked blunt bodies moving at high speed are conducted within the critical length of the spike. The author's previous work [13] included the study of forebody drag reduction methods from which the aerodisk-spike combination is found to be significantly reliable. A hemispherical body with a spike length greater than the critical spike length for flow at Mach 2.0 is tested, and up to a 20 % increase in the overall percentage of drag force reduction has been reported by mounting an intermediate aerodisk over the sharp tip spike stem in comparison with the conventional model. With the results obtained from their computational study, the authors reported that a further increase in drag reduction could be obtained for spike lengths exceeding the critical length by mounting an intermediated aerodisk over the spike stem. Sarwar et al. [14, 15] conducted a recent study focused on modifying the axisymmetric cavity formation between the spike tip head and the blunt base body to achieve drag reduction. The findings suggest that the alterations made in the study support drag reduction beyond the levels achieved with a conventional sharp spike. The incorporation of a spike on a blunt body with the intention of reducing drag introduces a notable chal–lenge in the form of flow instability. The intricacies of this flow instability, accompanied by its potential con–sequences, have been thoroughly explored [16-18]. Besides spiked bodies, numerous researches have been performed experimentally and computationally to ana–lyze the aerodynamic forces over different stream–lined bodies like cone, spiked, and ogive bodies [20-24]. More recently, the effect of spikes on the hemispherical body has been experimentally investigated at both supersonic as well as transonic speeds by Milicev [25]. More recently, researchers have performed unsteady computational work over spiked bodies and reported on the flow unsteadiness arising over these bodies [26-28].

In the present investigation, the authors have con–ducted a parametric study on the proposed spiked hemi–spherical model provided with an intermediate aerodisk mounted on the spike stem at the point of flow sepa–ration. The motivation of the present research is to investigate the variation in the amount of drag reduction with useful alterations of size and location of the inter–mediate aerodisk. The parametric study is performed by varying the size of the intermediate aerodisk as well as the location where the aerodisk will be mounted. The effect of geometrical alterations introduced in aerodisk-spike design is investigated by performing 2D axisy–mmetric computations for a freestream supersonic flow of Mach 2.0. The flowfield developed around the inter–mediate aerodisk mounted spiked blunt body models by changing the size and location of the intermediate aerodisk is computed, compared, and analyzed.

## 2. GEOMETRY

In present study, the dimensions of the model are kept similar to the model design introduced in the author's previous work (Tembhurnikar et al, 2020) except the location and size of the aerodisk. The hemispherical body is defined as having a main body diameter (D) of 15 mm and a length of 1.5D. All of the designs have a spike with a sharp tip, making a half-cone angle of 10 degrees from the neutral axis. Spike has 2 mm (0.12D) stem diameter and spreads beyond critical spike length for operating at Mach 2.0 with the ratio L/D=2.0. The location of mounting this intermediate aerodisk for the longest spike with an L/D ratio of 2.0 is considered at the flow separation point, which is observed at 17 mm from the spike tip. Further, two cases (variation in loca–tion and variation in size) have been implied to observe the parametric effect of an intermediate aerodisk on drag reduction. Figure 2 shows the geometric details of configurations considered for the current study.

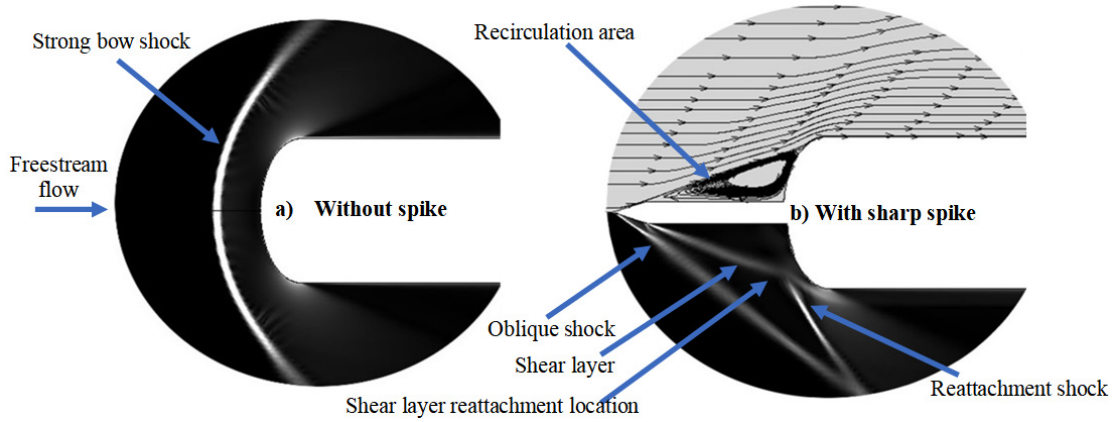


**Figure 1. Computed flow field over a typical blunt body without and with a spike [14].**

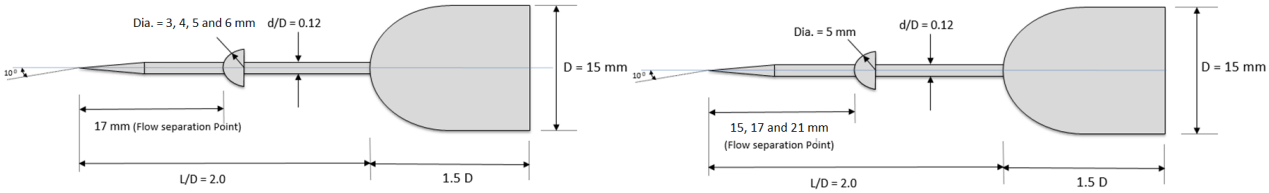


**A. Varying the size of intermediate aerodisk (Diameter: 3 mm, 5 mm and 6 mm)**

**B. variation in the location of aerodisk (at flow separation-17 mm, at pre-flow separation-15 mm, at post-flow separation-21mm)**

**Figure 2. Configuration of the parameteric models utilized in the present study**

## 3. COMPUTATIONAL METHODOLOGY

Steady-state two-dimensional axisymmetric computa–tions have been performed using ANSYS-FLUENT to study the flow over parametric models adopted in the present investigation. The solution methods comprise explicit formulation, Roe-FDS flux scheme, and gradient Green-Gauss cell-based spatial discretization with second-order upwind flow using the k-ω tur–bulence model. The Reynolds number is $3.5x10^5$ with respect to the forebody diameter of parametric models. The solver uses the finite volume approach to solve compressible Reynolds Averaged Naiver-Stokes equations. A typical grid with the computational do–main and boundary conditions adopted in the present investigation is presented in Figure 3. As shown in the figure, the inlet has been specified by pressure far-field boundary condition, the hemispherical body and spike are specified with no-slip wall boundary conditions, and the domain outlet is specified with pressure outlet. Following are the flow conditions applied for the simulations performed in the present research:

- Freestream Mach Number : 2.0
- Freestream Pressure: 39408.56 Pa
- Freestream temperature: 166.65 K
- Fluid Material / Working Fluid: Air (Ideal Gas)
- Fluid Viscosity: Sutherland

During the simulation, the residuals of continuity, energy and turbulent kinetic energy were monitored. In addition, the convergence history for drag was also monitored during the entire solution period. Results were analyzed only when it was ascertained that the residuals have converged to the order of $10^{-5}$. A wall $Y^+$ of less than 5 has been maintained in order to en–sure the correctness of the obtained numerical results.

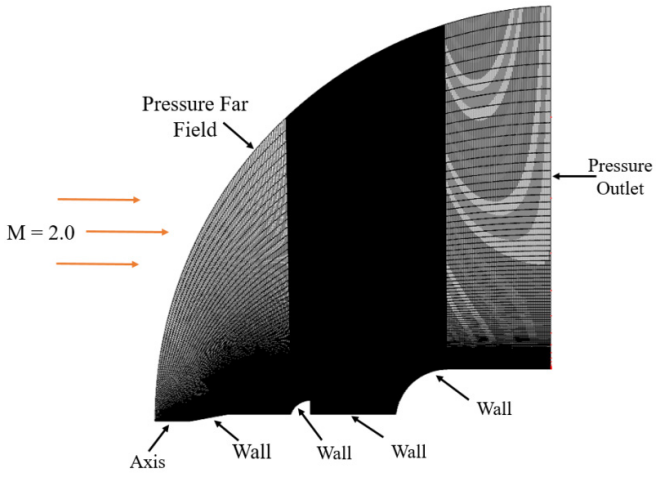


**Figure 3. Flow domain and boundary conditions adopted in the present study**

## 4. SOLVER VALIDATION, GRID INDEPDENDENCE AND TURBULENT MODELING

For the purpose of solver validation, the experimental study performed by J. T. White (1993) over a blunt body provided with a spike having ratio L/D=0.875 (L is the spike length and D is the main body diameter) at the supersonic flow of Mach M=2.23 has been taken into account. The validation work is also reported in the authors' previous literature (Tembhurnikar et al. 2020). The model adopted here is the blunt hemis–pherical body with a flat tip spike protruding from the blunt body's stagnation point. Figure 4 (A) shows the geometric specifics of the employed model for solver validation. The computational domain and the grid generated to conduct computations over the validation model are presented in Figure 4 (B). The surface pres–sure distribution computed over the forebody of the spiked hemisphere from the present computation is compared with the measured and computed surface pressure distribution data reported by J. T. White (1993). The comparison is shown in Figure 5. A fare agreement between the surface pressure distribution plots can be clearly seen in Figure 5 and thus validates the present solver. In order to converge to an appropriate grid and turbulence model, suitable grid independence study and turbulence modeling have been performed, respectively. Grids of various densities were adopted in order to perform the grid independence study, starting from a coarse grid of 30,000 cells to a fine grid of 1,20,000 cells. It was observed that on increasing the grid density, the results moved closer to the reported data, with the mesh consisting of 90,000 cells and 1,20,000 cells showing almost similar results and are in best agreement with the reported data, as can be seen in Figure 6A. Hence a grid with around 90,000 cells has been adopted for the present simulations. Similarly, in order to ensure the appropriate turbulence model for conducting the simulations in the present research, the validation case was simulated by taking various turbulence models (k- □, k-ω and Spalart almaras (S-A)) into consideration and the computed surface pressure distribution obtained from all the cases is compared in figure 6B. The figure shows that the surface pressure distribution computed by adopting the k-ω turbulence model provided the best result, which fairly matches the experimental data reported by J. T. White (1993). Hence, the k-ω turbulence model has been adopted in the present simulations.

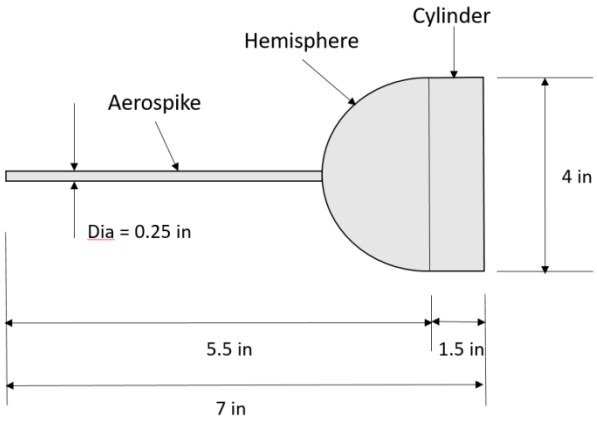


**A) Geometrical representation of spiked body adopted for validation**

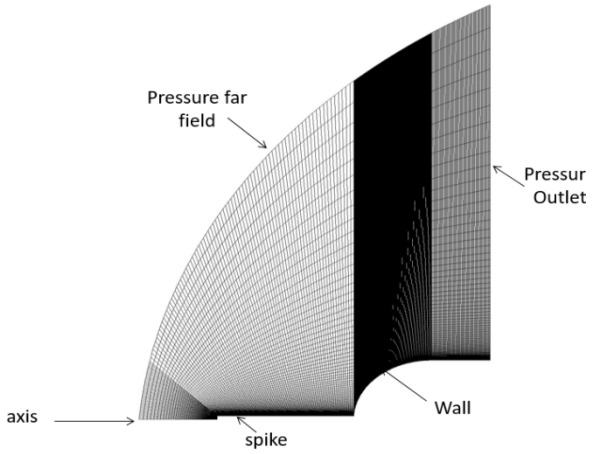


**B) Computational domain of validation model**

**Figure 4. Geometrical details and computational analysis domain of the model considered for solver validation**

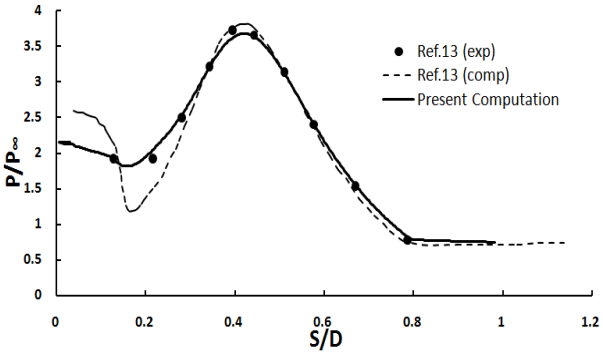


**Fig. 5. Comparison of time-averaged surface pressure distribution over the spiked hemisphere.**

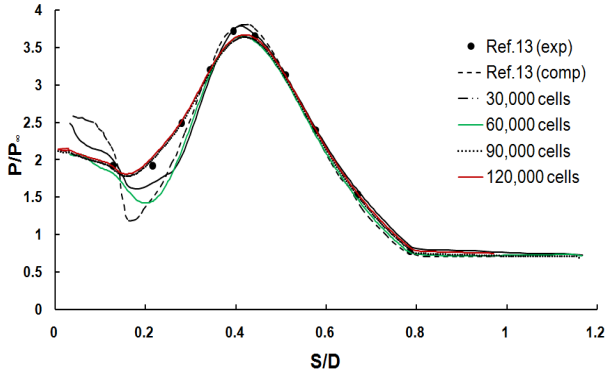


**A) Grid independence study**

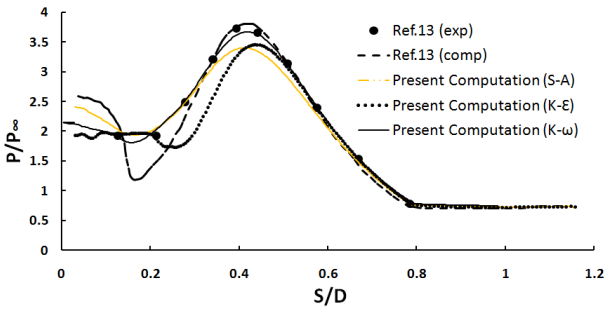


**B) Turbulence modeling**

**Fig. 6. Comparison of time-averaged surface pressure distribution over the spiked hemisphere for (A) Grid Inde–pendence Study and (B) Turbulence Modelling**

## 5. RESULTS AND DISCUSSION

To analyze the effect of parametric factors of the intermediate aerodisk on the flow field, the flow is simulated over a hemispherical body where an inter–mediate aerodisk is mounted on a sharp tip spike stem moving at freestream Mach 2.0. In this parametric study, the size of the aerodisk diameter varies from 3mm to 5mm and from 6mm. Also, the location of the aerodisk is varied as a pre-separation point (15mm from the sharp tip spike) and post-flow separation point (21mm from the sharp tip spike), keeping the diameter of the aerodisk as 4 mm. Each parametric model has a sharp tip spike of length to diameter ratio L/D = 2.0. The computational results of varying the location and size of the intermediate aerodisk mounted on the sharp tip spike stem of L/D ratio 2.0 are compared with the results obtained for the ideal spike-aerodisk-hemisphere combination reported in Tembhurnikar et al. (2020). The comparison is done based on the effect of the location and size of the aerodisk on the flow physics, pressure distribution over the model, and overall drag experienced. The major conclusions drawn from these comparisons are discussed in the following sub-sections.

### 6.1 Reattachment Shock Wave

The strength of reattachment shock is the major source of overall drag experienced by the main body. Flow characteristics developed around the blunt hemisp–herical body having sharp tip spike with intermediate aerodisk can be observed with the density contours of parametric models. Figure 7 represents the comparative density gradient contours of parametric models focusing on the effect of aerodisk size (Figure 7A) and the location of aerodisk at spike stem (Figure 7B).

Figure 7A and 7B illustrate the computed density gradients over the spiked body at a freestream Mach number of 2.0. These images reveal several flow phe–nomena resulting from the supersonic flow over a spiked body. Notable observations include the forma–tion of a shock wave at the spike tip, an expansion wave at the spike tip's edge, a bow shock wave due to the aerodisk, flow separation, the creation of a shear layer with a recirculation region, reattachment of the shear layer on the shoulder of the hemispherical blunt body, and the formation of a detached shock on the hemispherical blunt body due to the abrupt deflection of the flow over the body.

From Figure 7A, it is evident that the strength and position of the reattachment shock generated over the hemispherical forebody shoulder vary with changes in the size of the intermediate aerodisk. The thickness of the reattachment shock in the density gradient contour allows for a comparison of the shock strength in each case. For instance, with an aerodisk size of 3mm located 17mm from the spike tip (point of flow separation), the reattachment shock impacting the main body is less intense due to the smaller aerodisk size (Figure 7A(a)). Conversely, larger aerodisks (4mm, 5mm, and 6mm) result in a stronger separation shock at the aerodisk (Figure 7A(c) and (d)). Additionally, an increase in aerodisk diameter correlates with a larger recirculation region, as demonstrated in Figure 7A(a-d).

Figure 7B (a-c) shows that changing the aerodisk's location also affects the reattachment shock's intensity and alters the recirculation region. Specifically, placing an intermediate aerodisk before the flow separation point results in a reattachment shock with minimal strength compared to other aerodisk positions (at flow separation and post-flow separation). When the intermediate aerodisk is positioned after the flow separation point, the reattachment shock wave impacting the hemispherical body is of higher intensity due to the increased flow turn angle relative to the original model geometry (Figure 7B(c)).

### 6.2 Recirculation zone

The formation of the recirculation region, with its shape and size, directly impacts the reduction in drag force on the spiked body. Figures 8A and 8B illustrate the flow phenomena within the recirculation region using streamlined contours. Configuration changes, whether by varying disk diameters or altering disk locations on the spike, result in different flow patterns.

Figure 8A(a), which illustrates a 3mm disk diameter, shows a single recirculating vortex. As the disk diameter increases, both the number and size of recirculating vortices increase. For a 4mm disk diameter, one vortex forms near the blunt body surface while another smaller vortex forms near the disk's edge. When the disk diameter increases from 5mm to 6mm, the size of the secondary recirculation vortex grows, which may contribute to a reduction in the drag force on the spiked body.

Figure 8B provides comparative details of the recirculation regions for various parametric models, illustrating the effects of changing the disk's location on the spike stem in a supersonic flow of Mach 2.0. An intermediate aerodisk with a diameter of 4mm, mounted before the point of flow separation, exhibits a relatively larger recirculation region and a less intense reattachment shock (Figure 8B(a)).

Conversely, if the aerodisk is mounted past the flow separation point (Figure 8B(c)), it reduces the drag force on the hemispherical blunt body less effectively. A reduced recirculation area is observed for the hemispherical blunt body with the intermediate spike located post-flow separation, and the reattachment shock is stronger. This change in the flow characteristics can lead to a less significant reduction in the drag force compared to other disk location arrangements. With the analysis made based on the qualitative results as mentioned in the present and previous subsections, it is evident that the size and location of the intermidiate aerodisk will have an impact on the pressure distribution and the forebody drag coefficients experienced by the spiked body. The quantitative data computed in the present investigation is reported in the next sub-sections.

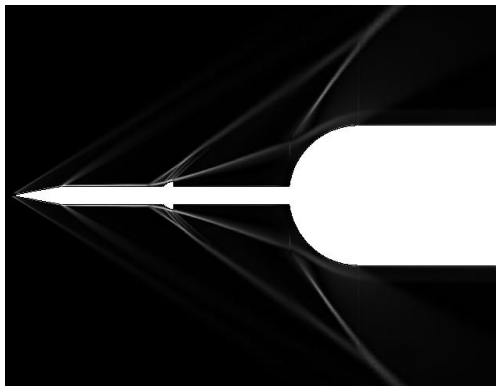

a) Dia 3

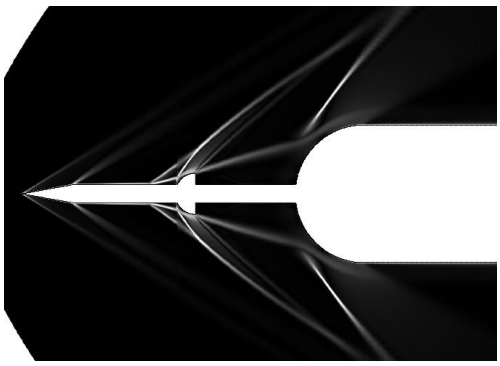

b) Dia 4

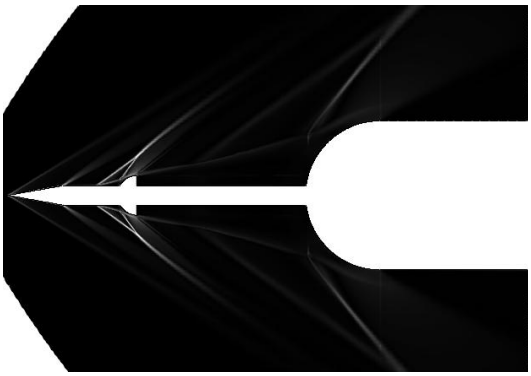

a) Pre-separation

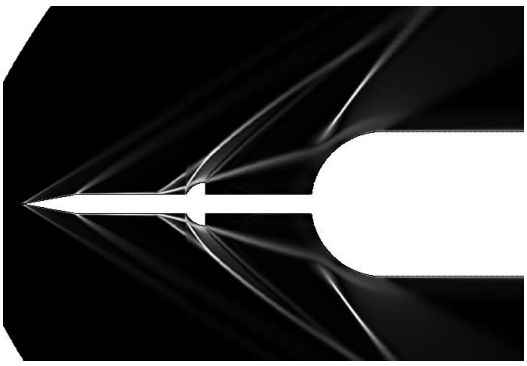

b) At-separation

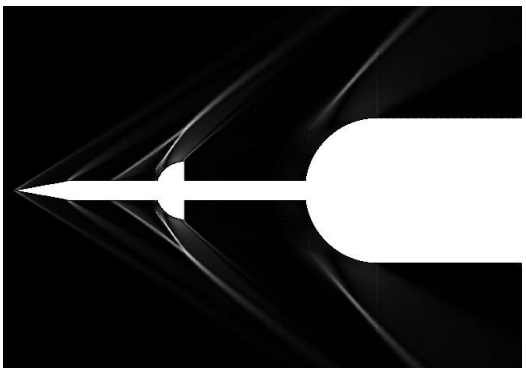

c) Dia 5

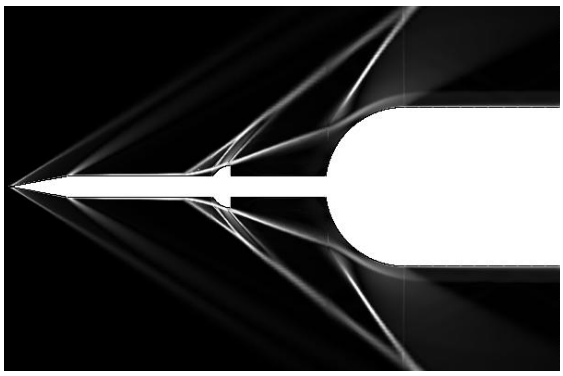

c) Pre-separation

B) Variation in Aerodisk Location

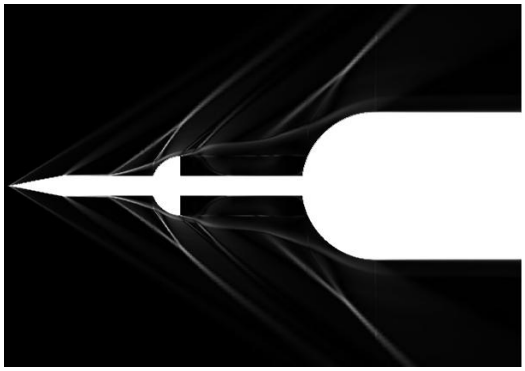

d) Dia 6

A) Variation in Aerodisk Size

Figure 7 Comparisons of Contours of Density Gradient

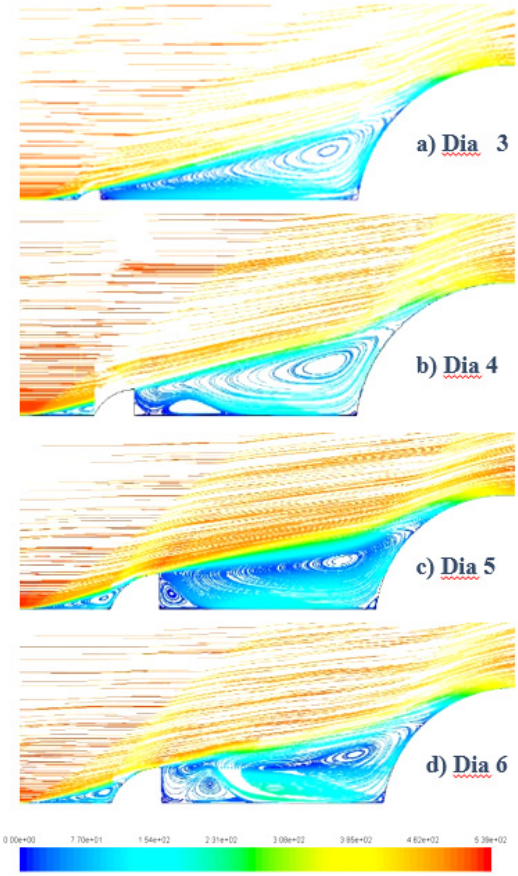


A) Variation in Aerodisk Size

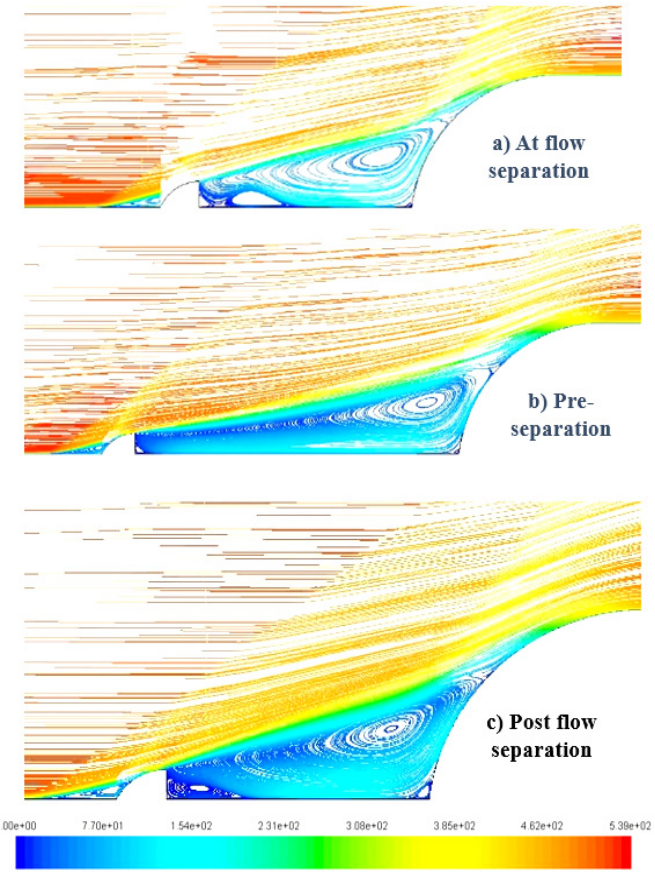


B) Variation in Aerodisk Location

Figure 8 Velocity Streamlines over parametric models

Figure 9 shows the effect of intermediate aerodisk size (Figure 9A) and location (Figure 9B) on the surface pressure distribution over the forebody. Along the hemispherical forebody surface, a gradual increase in the pressure is seen and pressure peak is observed at the flow reattachment point where the reattahcment shock generates. Parametric models having aerodisk diameter 5mm and 6mm have this reattachment shock a little later than the other two cases. The early presence of a shock wave (3mm case) means the shock wave has a higher flow turn angle and, hence, increased shock strength. The higher the peak, the fiercer the shock wave. Hence, a higher pressure coefficient peak is observed for the 3mm case (see Figure 9A). For reattachment shock waves at the hemispherical body, a model with an aerodisk diameter of 5 mm has the lowest pressure coefficient value. The strength of reattachment shock is the major source of drag. This reattachment shock at the main body mutually contributes to elevated drag value.

Figure 9B presents the comparison of surface pressure distribution curves over forebody parametric models varying in the location of intermediate aerodisk on the spike stem of ratio L/D = 2.0. The pressure rise for each case is due to presence of reattachment shock wave at the forebody. For the aerodisk mounted at a location before the flow separation point, the reattachment shock is less intense as compared to the other two cases.

Models with aerodisk positioned at flow separation and after flow separation has reattac–hment shock of the minimal variation in strength, but higher compared to the third case with aerodisk moun–ted prior to the flow separation point. A parametric model with aerodisk-mounted pre-flow separation (15 mm from spike tip) reports significantly lower peak pressure coefficient values for the reattachment shock wave. From Figure 9B, it has been observed the for–mation of reattachment shock for the parametric models with the location of intermediate aerodisk at the separation point and post-separation point is delayed in comparison to the case with intermediate aerodisk located at the separation point.

### 6.3 Forebody drag

The points discussed in the above subsections all add to the reason for the overall drag experienced by the body. The system of shock waves, their position and strength of shock waves, the area of recirculation region, and the pressure distribution over a body kept in a flow all contribute to the foredrag values of that body. The reattachment shock wave strength is of main concern. Overall drag is composed of pressure drag and skin friction drag. The change in the modifications to the geometry is mainly influenced by the pressure drag (see Figure 10). The drag coefficients obtained by simulating the flow over spiked-aerodisk-body geometries studied in the present study are specified in Table 1.

From Table 1 and Figure 10, a parametric model with an aerodisk diameter of 4 mm mounted before flow separation at a distance of 15 mm from the sharp spike tip has the lowest overall drag till now. As the aim of the present research is to investigate drag reduction methods, a model with an aerodisk mounted on a spiked stem before flow separation is the most reliable. For variation in intermediate aerodisk size, a model with an aerodisk diameter of 5 mm reported the minimum forebody drag coefficient. On the above aspect, a variation in the forebody drag coefficient values is expected to be observed with a change in the size and location of the intermediate aerodisk. The details of the computed forebody drag coefficient are reported in the next sub-section.

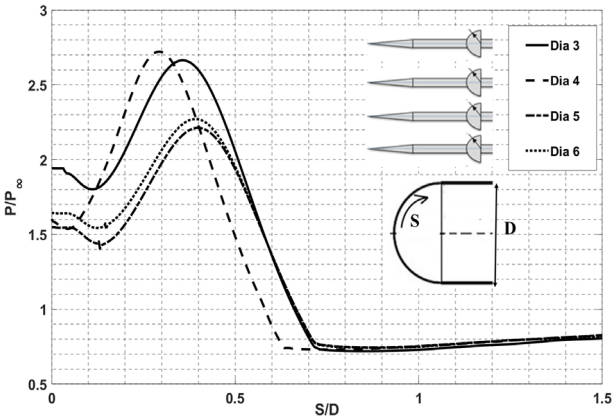


**A) Variation in Aerodisk Size**

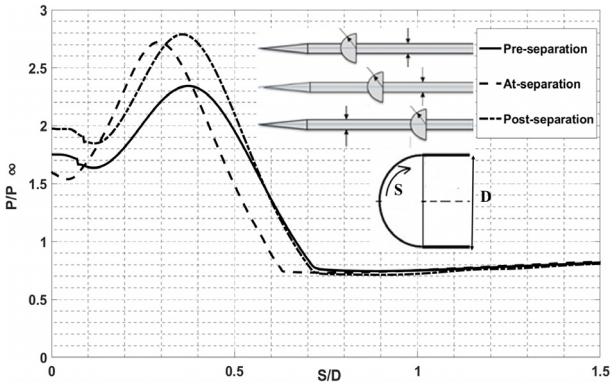


**B) Variation in Aerodisk Location**

**Figure 9 Computed surface pressure distributions over the parametric models with variation in (A) aerodisk size and (B) location of intermediate aerodisk at spike stem.**

**Table 1. Forebody drag obtained for studied parametric models**

| Model | Coefficient of Drag ($C_d$) | | |
|---|---|---|---|
| | Pressure | Skin Friction | Total |
| Effect of Aerodisk Diameter | | | |
| 3 mm | 0.405 | 0.018 | 0.422 |
| 4 mm | 0.381 | 0.022 | 0.403 |
| 5 mm | 0.315 | 0.011 | 0.326 |
| 6 mm | 0.342 | 0.011 | 0.352 |
| ***Effect of Location of Intermediate Aerodisk (for Aerodisk Diameter 4 mm)*** | | | |
| At Pre-Flow Separation (15 mm) | 0.344 | 0.016 | 0.361 |
| At Separation Location (17mm) | 0.381 | 0.022 | 0.403 |
| At Post Flow Separation (21 mm) | 0.415 | 0.018 | 0.433 |

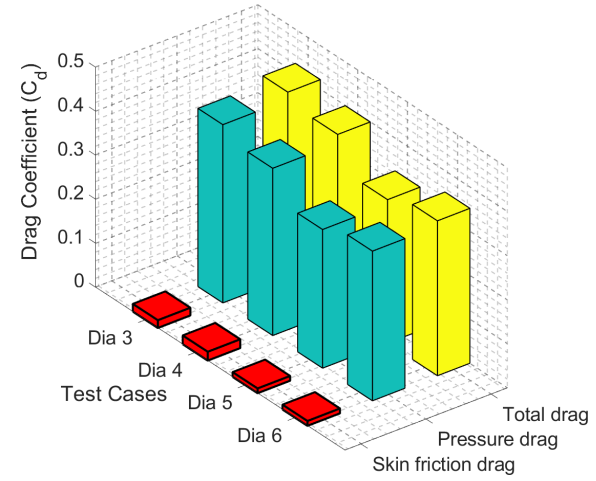


**A) Variation in Aerodisk Size**

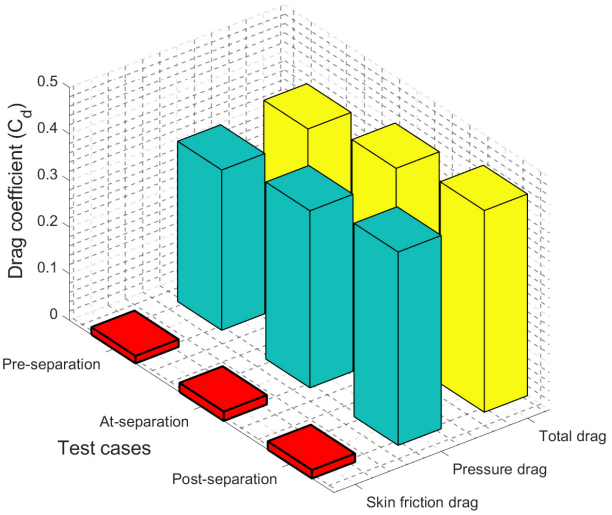


**B) Variation in Aerodisk Location**

**Figure 10 Computed forebody drag values over the para–metric models with variation in (A) aerodisk size and (B) location of intermediate aerodisk at spike stem.**

## 6. CONCLUSION

Apart from the additional weight, mounting an inter–mediate aerodisk at the sharp tip spike stem of length increased beyond critical length is found to be very significant. The author's previous work reported up to 20% additional reduction in forebody drag values in comparison to the conventional spike-body configu–ration moving at a supersonic speed of Mach 2.0 [13]. In order to investigate the efficacy of the intermediate aerodisk, a parametric analysis was performed in two sections, i.e. variation in aerodisk size and variation in location of aerodisk on the spike stem. The strength of the reattachment shock wave hitting the hemispherical body, the recirculation area between the aerodisk and main body, and effective pressure distribution over the body are the aspects decisive of the overall drag reduction. Major findings deduced from the present research from such aspects are as follows:

**Effectiveness of Intermediate Aerodisk:** The addi–tion of an intermediate aerodisk was found to influence the flow field around the forebody significantly. The size of the recirculation zone was increased by strate–gically placing the aerodisk, particularly before the po–int of flow separation. This enlargement of the recir–culation region effectively reduced the strength of the reattachment shock, leading to lower surface pressure levels and ultimately achieving drag reduction.

**Parametric Analysis:** Parametric models with var–ying aerodisk sizes (3mm, 5mm, and 6mm) and loca–tions (pre and post flow separation point) were ana–lyzed. Results indicated that reducing the size of the aerodisk to 3mm maintained identical reattachment shock strength but led to higher pressure values at the transition from separation shock to reattachment shock. Conversely, an expanded 5mm aerodisk size exhibited improved flow recirculation, resulting in lower peak pressure coefficients for the reattachment shock and reduced heating levels.

**Impact on Drag Reduction:** The study emphasized that the strength of the reattachment shock is the primary source of overall drag experienced by the fore–body. Models with an intermediate aerodisk diameter of 4mm mounted before the flow separation point reported the lowest overall drag coefficients. Additionally, the model with a 5mm aerodisk diameter exhibited the minimum forebody drag coefficient, suggesting that this configuration provides an optimal balance between flow recirculation and reattachment shock strength.

**Optimal Configuration:** The research concludes that incorporating an intermediate aerodisk, particularly with a diameter of 5mm and mounted before the flow separation point, offers the most reliable method for drag reduction in high-speed flying vehicles operating at Mach 2.0. This configuration effectively enhances flow recirculation, reduces reattachment shock strength, and minimizes overall drag, thereby contributing to imp–roved aerodynamic performance and efficiency.

As the 5 mm diameter aerodisk proved to be the best configuration among the cased studied in the present investigation, future research work can be carried out on the best location keeping 5 mm as the aerodisk size. Furthermore, 3D approach and non-zero angles-of-at–tack could also be considered and in addition the effect of intermediate aerodisk over the flow insteadiness arising over the spiked body can also be investigated in future.

## REFERENCE

[1] Crawford, D. H.: Investigation of flow over a spiked nose hemisphere cylinder at Mach number of 6.8, NASA-TND-118, December 1959.

[2] Ahmed, M. Y.M., Qin, N.: Recent advances in the aerothermodynamics of spiked hypersonic vehicles, Progress of Aerospace Sciences, vol. 47, 425-499 (2011).

[3] Jones J.: Flow Separation from Rods Ahead of Blunt Noses at Mach number 2.72, NACA RM L52E05a (1952).

[4] Yamauchi M., Fuji K., and Higashino F.: Numerical Investigation of Supersonic Flow around a Spiked Blunt Body, Journal of Spacecraft and Rockets, vol. 32, no. 1, pp. 32–42 (1995).

[5] Das S., Kumar P., Prasad J.K., Ralh M.K., Rao R.K.M.: Drag Reduction of a Hemispherical Body

adopting Spike at Supersonic Speed, Journal of Aerospace Science, vol. 65, no. 4, pp. 313–325 (2013).

[6] Sahoo D., Das S., Kumar P., and Prasad J.: Effect of spike on steady and unsteady flow over a blunt body at supersonic speed, Acta Astronautica, vol. 128, pp. 521–533 (2016).

[7] Sarwar, G., Kumar, P., & Das, S.: Flow field characteristics of a blunt body with different nose cone fairing at supersonic speed. In *Conference on Fluid Mechanics and Fluid Power* (pp. 389-393). Singapore: Springer Nature Singapore, 389-393. (2021)

[8] Sarwar, M. G., Kumar, P., & Das, S.: Influence of Nose Cone Fairing and Spike on Supersonic Blunt Body Flows. Journal of Spacecraft and Rockets, 1-17. (2023).

[9] Menezes V., Saravanan S., Jagadeesh G., Reddy K.P.J.: Experimental investigations of hypersonic flow over highly blunted cones with aerospikes, AIAA Journal, vol. 41, no. 10, pp. 1955–1966 (2003).

[10] Milicev, S. S., Pavlovic, D. M.: Influence of spike shape at supersonic flow past blunt nosed bodies: experimental study, AIAA Journal. Vol. 40, issue 5, 1018–1020 (2002).

[11] Yadav, R., Guven, u.: Aerothermodynamics of a hypersonic projectile with a double-disk aerospike, Aeronautical Journal, vol. 117, no. 1195, 913–928 (2013).

[12] Yadav, R., Velidi, G., Guven, u.: Aerothermody–namics of generic reentry vehicle with a series of aerospikes at nose, Acta Astronauta, vol. 96, 1–10 (2014).

[13] Tembhurnikar P., Jadhav A., Sahoo D.: Effect of Intermediate Aerodisk Mounted Sharp Tip Spike on the Drag Reduction over a Hemispherical Body at Mach 2.0, FME Transactions, vol.48, 2020.

[14] Sarwar, M.G., Kumar, P., & Das, S.: Insight into the mechanism of drag reduction for a spiked blunt body. In Aerospace and Associated Technology, Routledge, 71-76. (2022).

[15] Sarwar, M. G., Kumar, P., Das, S. (2023). Supersonic flow investigation of a drag reducing conical spike on a hemispherically blunted nose body. Proceedings of the Institution of Mechanical Engineers, Part G: Journal of Aerospace Engineering, vol. 237, no. 9, 1992-2007 (2023).

[16] Sahoo, D., Karthick, S. K., Das, S., Cohen, J.: Parametric Experimental Studies on Supersonic Flow Unsteadiness over a Hemispherical Spiked Body, AIAA Journal, vol. 58, no. 8, 3446–3463 (2020)

[17] Sahoo, D., Karthick, S. K., Das, S., and Cohen, J.: Shock-Related Unsteadiness of Axisymmetric Spiked Bodies in Supersonic Flow, Experiments in Fluids, vol. 62, no. 4, 1–21 (2021)

[18] Sugarno, M. I., Sriram, R., Karthick, S. K., Jagadeesh, G.: Unsteady Pulsating Flowfield over Spiked Axisymmetric Forebody at Hypersonic Flows, Physics of Fluids, vol. 34, no. 1, 2022, 016104 (2022)

[19] White, J. T.: Application of Navier–Stokes Flowfield Analysis to the Aero-thermodynamic Design of an Aerospike-Configured Missile, AIAA, 0968 (1993).

[20] Damljanović, D., Rašuo, B.: Testing of Calibration Models in Order to Certify the Overall Reliability of the Trisonic Blowdown Wind Tunnel of VTI, FME Transactions, Vol. 38, No. 4, pp. 167-172, 2010.

[21] Samardžić, M., Isaković, J., Miloš, M., Anasta–sijević, Z., and Nauparac D. B.: Measurement of the Direct Damping Derivative in Roll of the Two Callibration Missile Models, FME Transactions, Vol. 41, pp. 189-194, 2013.

[22] Tarakka R., Salam, N., Jalaluddin, and Ihsan H.:Effect of Blowing Flow Control and Front Geometry Towards the Reduction of Aerodynamic Drag on Vehicle Models, FME Transactions, Vol. 47, pp. 552-559, 2019.

[23] Gholap, T.B., Salokhe, R.V., Ghadage, G.V., Mane, V., and Sahoo, D.: Aerodynamic Analysis of an AK-47 Bullet Moving at Mach 2.0 in Close Proximity to the Ground, FME Transactions, Vol.50, No. 2, pp. 369-381, 2022.

[24] Salunke, S., Shinde, S., Gholap, T., and Sahoo, D.: Comparative Computational Analysis of NATO 5.56 mm, APM2 7.62 mm and AK-47 7.82 mm Bullet Moving at Mach 2.0 in Close Vicinity to the Wall, FME Transactions, vol.51, No. 1, pp. 81-89, 2023.

[25] Milićev, S. S.,: An Experimental Study of the Influence of Spike in Supersonic and Transonic Flows Past a Hemispheric Body, FME Transactions, Vol. 50, No. 1, 2022, pp. 24-31

[26] Wei Cui, Jinglei Xu, Bing-Chen Wang.: Large-eddy simulation of unsteady flows past a spiked body, Acta Astronautica, Volume 213, 2023, Pages 277-294.

[27] Wang Y, Xu J, Qin Q, Guan R, Cai L. Experimental Investigation of the Shock-Related Unsteadiness around a Spiked-Blunt Body Based on a Novel DMD Energy Sorting Criterion. *Aerospace*. 2024; 11(3):188.

[28] Bibin John, Michal Jan Geca, Surya Saravanan, Dathi S.N.V. Rajasekhar Rao: Unsteady wave drag reduction in hypersonic flows: Correlations and influences of pulsed energy magnitude and deposition location, Aerospace Science and Technology, Volume 144, 2024

---

**УТИЦАЈ ВЕЛИЧИНЕ И ЛОКАЦИЈЕ СРЕДЊЕГ АЕРОДИСКА ПОСТАВЉЕНОГ ОШТРОГ ВРХА НА СМАЊЕЊЕ ОТПОРА ПРЕКО ХЕМИС–ФЕРИЧНОГ ТЕЛА ПРИ БРЗИНИ ОД 2.0 МАХА**

**А.Т. Јадхав, П.В. Тембурникар, М.Б. Босхале, Ј. Нанди, М.Д.Г. Сарвар, Д. Саху**

Да би се смањио отпор предњег тела у летећим возилима велике брзине као што су пројектили и ракете, савремена истраживања су се фокусирала на рачунарске методе за анализу стратегија смањења отпора. Ова студија истражује ефикасност средњег аеродиска постављеног на шиљак са оштрим врхом при Маховом броју од 2.0. Кроз параметарску анализу, истражују се варијације у величини аеродиска и локацији на стаблу шиља. Резултати показују да смањење величине средњег аеродиска на 3 мм одржава идентичну снагу ударца при поновном причвршћивању, али доводи до виших вредности притиска на прелазу из шока раздвајања у удар поновног причвршћивања. Модел са проширеном величином аеродиска од 5 мм показује други најнижи коефицијент вршног притиска за шок поновног причвршћивања, што сугерише побољшану рециркулацију протока и ниже нивое грејања. Насупрот томе, величина аеродиска од 6 мм повећава ударни притисак при поновном причвршћивању, али побољшава рециркулацију протока, утичући на укупни отпор. Све у свему, студија закључује да средњи аеродиск, посебно пречника 5 мм, пружа оптималну конфигурацију за смањење отпора пре одвајања протока.